



A New Generation Buck–Boost and Flyback DC–DC Converter

Ch. Kranthi Kumar, Dr. G.Jaya Krishna

M. Tech Student, Dept. of Electrical and Electronics Engineering, NEC, Gudur, AP, India

Professor & HOD, Dept. of Electrical and Electronics Engineering, NEC, Gudur, AP, India

ABSTRACT: This paper present non isolated and isolated soft-switched dc–dc topologies with the step-up/down ability. The non isolated topology is made by adding a tiny ac capacitor in parallel with the most electrical device of the standard buck–boost device and exchange its semiconductor devices with the reverse-blocking switches. By employing a novel management theme, true zero-voltage switch is accomplished at each input and turn-off of the ability switches regardless of the input voltage, output voltage, or load worth. The isolated type of the device is made by substituting the most electrical device with Associate in Nursing air gapped high-frequency transformer, like the fly back device. During this case, two smaller ac capacitors area unit placed on either side of the electrical device to comprehend soft switch further as passive clamping no additional clamping circuit is needed. the essential operation of the projected partial-resonant converters includes four modes and is delineate well. The comprehensible analysis of the topologies is dispensed further. Using simulink leads to completely different operative conditions area unit provided to verify the performance of the projected power converters.

KEYWORDS: Air-gapped transformer, dc–dc converter, resonant power conversion, soft switching.

I. INTRODUCTION

A new generation of soft-switched buck–boost dc–dc converters was introduced in this project. The partial-resonant network is composed of a small inductor in parallel with a small ac capacitor. The main role of the inductor is to transfer power by charging from the input and discharging to the output or vice versa. The parallel capacitor creates partial resonances to realize zero-voltage turn-on and turn-off for the converter's switches. The inductor can be simply replaced by an air-gapped high- frequency transformer to achieve galvanic isolation. In the innovative nonisolated and isolated soft-switched dc–dc topologies with the step-up/down ability. The nonisolated topology is constructed by adding a small ac capacitor in parallel with the main inductor of the conventional buck–boost converter and replacing its semiconductor devices with the reverse-blocking switches. By using a novel control scheme, true zero-voltage switching is realized at both turn-on and turn-off of the power switches irrespective of the input voltage, output voltage, or load value. The isolated form of the converter is created by substituting the main inductor with an air-gapped high-frequency transformer, similar to the flyback converter. In this case, two smaller ac capacitors are placed on both sides of the transformer to realize soft switching as well as passive clamping; no extra clamping circuit is required. Before this Pulse width modulated (PWM) dc–dc power converters are well developed and are widely used. These converters are simple and relatively low cost. However, PWM topologies have the disadvantages of considerable switching losses, high switching stresses, and significant electromagnetic interference due to the hard-switching operation. Soft-switching topologies incorporating zero-voltage and zero-current switching have been introduced to increase the conversion efficiency, switching frequency, and power density of converters. Several soft-switching dc–dc topologies have been proposed in the literature; they can be mainly categorized as quasi-resonant, multi resonant, resonant-transition, active-clamp, phase-controlled, and resonant-load converters. By moving the switching frequency closer to or further from the resonant frequency of the tank network, the load voltage can be controlled. According to the formation of the resonant network, resonant-load converters can also be subdivided as series resonant, parallel resonant, series-parallel LCC resonant, and LLC topologies. Care should be taken in the consideration of various soft-switching dc–dc converters; Several introduced resonant converters have noticeable drawbacks besides their soft-switching privileges. The drawbacks include poor performance over a wide range of input voltages and load resistances, poor efficiency at the light load due to current circulation in the tank elements, increased conduction losses, and high device voltage stress.

International Journal of Advanced Research in Electrical, Electronics and Instrumentation Engineering

(An ISO 3297: 2007 Certified Organization)

Vol. 5, Issue 7, July 2016

The soft-switched partial-resonant dc–dc converters in the isolated and non-isolated configurations are introduced in this paper based on the authors’ previous work on the resonant ac-link converters. The non-isolated topology is the new reformation of the conventional buck–boost converter with the advantage of soft switching. An ac capacitor and two reverse-blocking (RB) switches are added to achieve this benefit. Compared to the quasi-resonant converters, the true ZVS happens in the proposed topology at both turn-on and turn-off of all the semiconductor devices regardless of the load level and voltage values. Galvanic isolation can be realized by employing an air-gapped high-frequency transformer similar to the fly-back converter without any snubber circuitry.

II. PROPOSED BUCK-BOOST AND FLYBACK DC-DC CONVERTER

The basic new generation limit resonant buck–boost dc–dc converter is proposed in Fig. 1(a). Similar to the conventional buck–boost

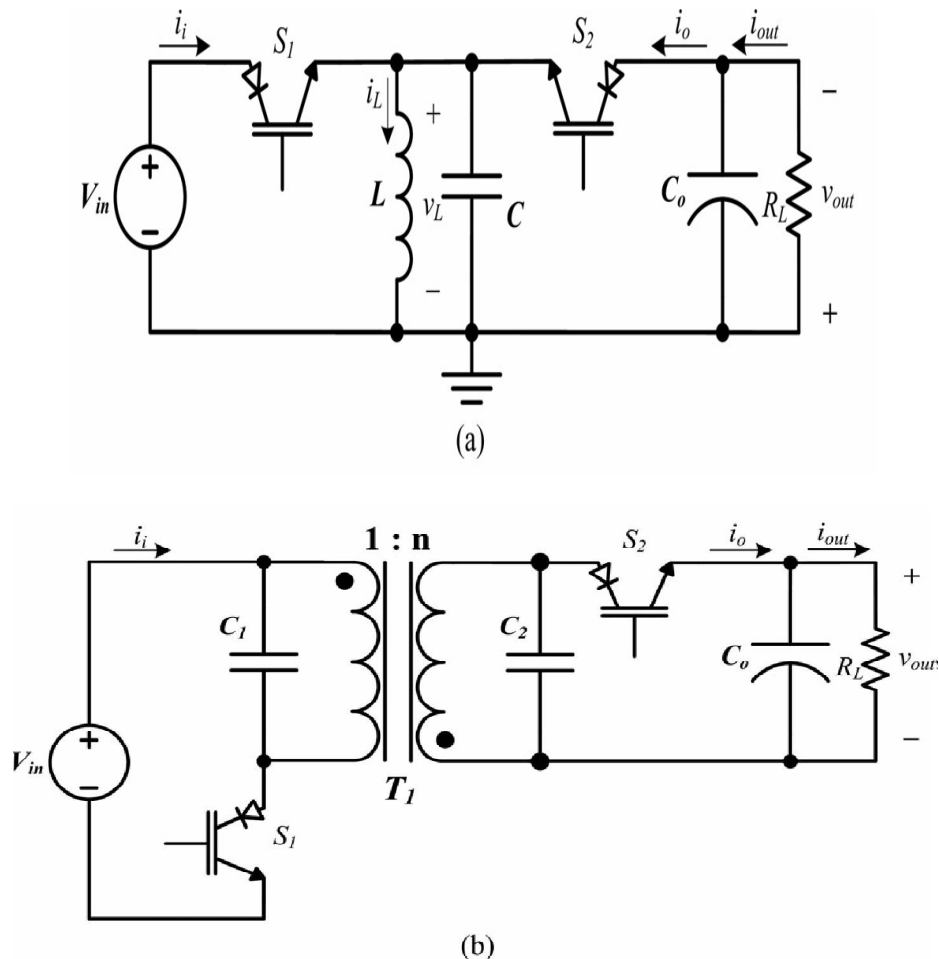


Fig.1. Proposed partial-resonant dc–dc converters. (a) Nonisolated buck– boost topology, and (b) isolated flyback topology.

converter, inductor L is responsible for transferring power from the input to the output. This inductor is charged from the input and then discharged to the output cycle-by-cycle. Small ac capacitor C is placed in parallel with this inductor. The main role of capacitor C is to produce partial resonances with the inductor to realize ZVS for the power devices, as will be shown later. As the figure depicts, the converter needs two (RB) switches. An RB-switch can be realized by a

International Journal of Advanced Research in Electrical, Electronics and Instrumentation Engineering

(An ISO 3297: 2007 Certified Organization)

Vol. 5, Issue 7, July 2016

conventional reverse-conducting switch (IGBT or MOSFET) in the series with a diode. However, the newly available individual RB-switches can be employed with the advantage of lower total on-state voltage.

Fig. 1(b) shows the isolated topology. In this converter, the magnetizing inductance of the high-frequency transformer is used for transferring power. In order to reach an appropriate inductance value, the transformer may need to have an air gap. Two smaller capacitors, C_1 and C_2 , provide partial resonance. These capacitors are placed on both sides of the transformer to also provide paths for the currents of the primary and secondary leakage inductances and subsequently, avoid voltage spikes when the input and output switches are turned OFF. As a result, no extra snubber circuit is required.

III. PRINCIPLE OF OPERATION

The operation of the proposed soft-switched dc–dc converter in both nonisolated and isolated configurations is composed of four modes in each switching cycle. The converter’s main inductance charges through the input in mode 1 and discharges to the output in mode 3. Modes 2 and 4 are for partial resonance of the main inductance with its parallel capacitance to achieve ZVS at both turn-on and turn-off of the power switches. A typical switching cycle of the isolated partial-resonant topology is shown in Fig. 2, and its corresponding operating modes are shown in Fig. 3. The state-plane diagram is also depicted in Fig. 4. The detailed operating modes of the isolated converter are explained in detail as follows by ignoring the transformer’s leakage inductances and winding resistances. Their effects will be shown later.

A. Mode 1 [Inductance Charges From the Input, Fig. 3(a)]

Switch S_1 is turned ON to connect the input dc voltage across the magnetizing inductance of the transformer, L_M . As a result, L_M charges in the positive direction. This mode is allowed to run until the average of the input current meets the input reference current, I_i^* . Subsequently, switch S_1 is turned OFF.

Note that due to the existence of capacitors C_1 and C_2 , the magnetizing inductance voltage, $v_L(t)$, decreases slowly when switch S_1 is turned OFF. As a result, the voltage of switch S_1 goes up slowly its turn-off in

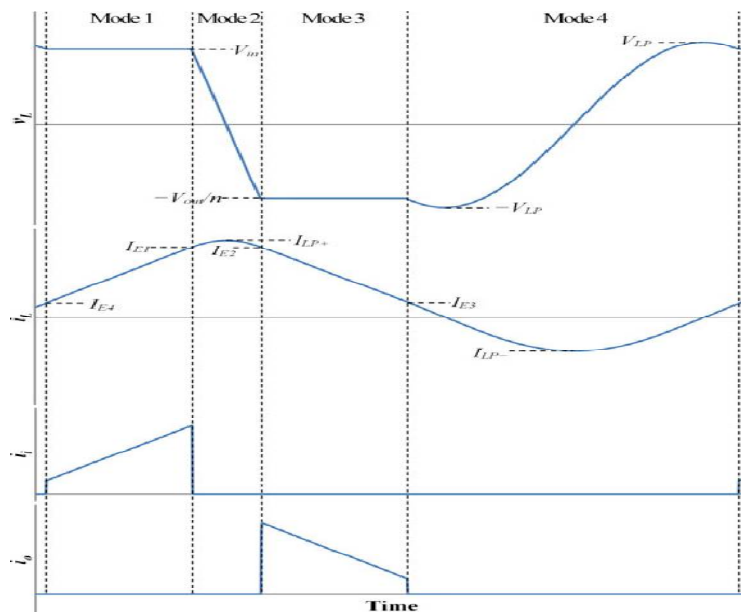


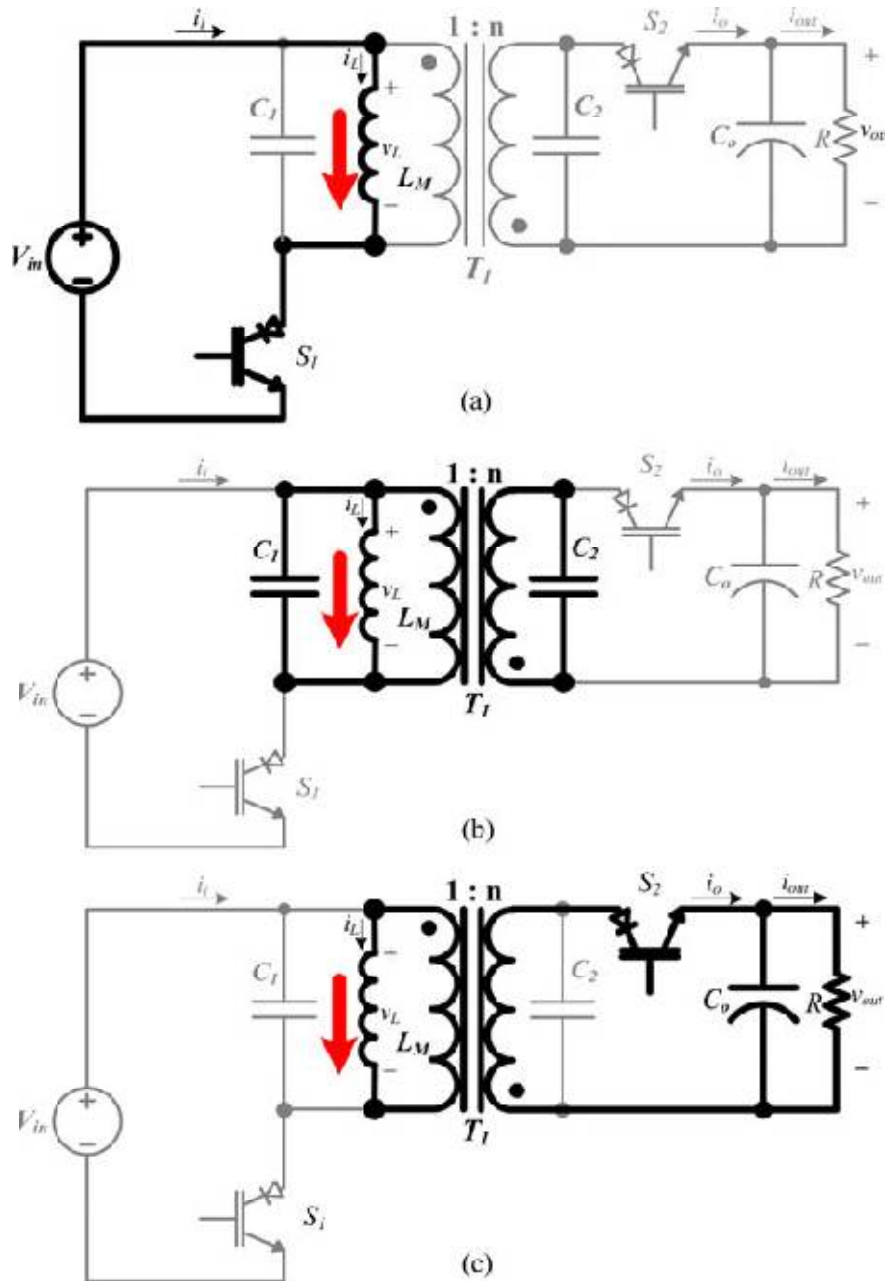
Fig. 2. Waveforms of the proposed isolated converter. (a) Magnetizing inductance voltage, (b) magnetizing inductance current, (c) input current, and (d) output current.

International Journal of Advanced Research in Electrical, Electronics and Instrumentation Engineering

(An ISO 3297: 2007 Certified Organization)

Vol. 5, Issue 7, July 2016

transition. Therefore, the turn-off of switch S_1 occurs at almost zero voltage. Switch S_2 has a similar ZVS in its turn off. As the ZVS behavior at the turn-off of the power switches is caused by the existence of C_1 and C_2 , it happens at any input voltage, output voltage, or load value.



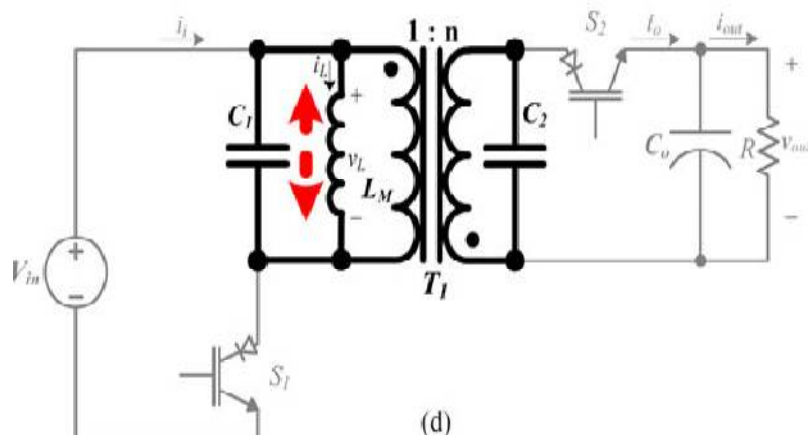


Fig.3. Operating modes of the proposed isolated partial-resonant converter.(a) Mode 1, (b) mode 2, (c) mode 3, (d) mode 4.

B. Mode 2 [Partial Resonance, Fig. 3(b)]

L_M starts to partially resonate with its total parallel capacitance, $C_t = C_1 + n^2 C_2$ (n is the transformer's turns ratio), and therefore, $v_L(t)$ starts to drop. This partial resonance is permitted to run until $v_L(t)$ becomes equal to the output reflected voltage ($-V_{out}/n$), which then allows the converter to go to mode 3 with soft transition. During this mode, the magnetizing inductance current, $i_L(t)$, reaches its positive peak value, I_{LP+} .

C. Mode 3 [Inductance Discharges to Output, Fig. 3(c)]

The load-side switch, S_2 , is turned ON to discharge the magnetizing inductance energy to the output. This mode continues until $i_L(t)$ reaches a small value of I_{E3} , which will be defined later. After that, this mode ends and switch S_2 turns OFF. In order to leave a certain amount of current in L_M at the end of mode 3 in the digital control implementation, $i_L(t)$ is constantly measured. Once $i_L(t)$ reaches the desired value, switch S_2 is turned OFF and the converter goes to mode 4.

The magnetizing inductance voltage is equal to the output reflected voltage at the beginning of mode 3 when switch S_2 is turned ON. As a result, the turn-on transition of switch S_2 occurs at zero voltage. The zero-voltage turn-on also happens for switch S_1 similarly. This ZVS at the turn-on of the power switches does not depend on the load level and voltage values.

D. Mode 4 [Partial Resonance, Fig. 3(d)]

L_M and C_t resonate together again. This considerable partial resonance is maintained until $v_L(t)$ is equal to the input voltage in the down-going direction, which then permits the converter to go to mode 1 with soft transition. Therefore, $v_L(t)$ should go higher than the input voltage during this mode as shown in Fig. 2. In the case that V_{out}/n is more than the input voltage, this process happens naturally, and I_{E3} can be selected as zero (the peak value of the magnetizing inductance voltage, V_{LP} , will be equal to V_{out}/n). However, when V_{out}/n is smaller than the input voltage, a certain amount of current should be left in the magnetizing inductance at the end of mode 3 to force $v_L(t)$ to peak higher than the input voltage as follows: where V_{LP} is the predetermined peak value of the magnetizing inductance voltage and can be selected to be 10% to 15% higher than the input voltage in practice.

International Journal of Advanced Research in Electrical, Electronics and Instrumentation Engineering

(An ISO 3297: 2007 Certified Organization)

Vol. 5, Issue 7, July 2016

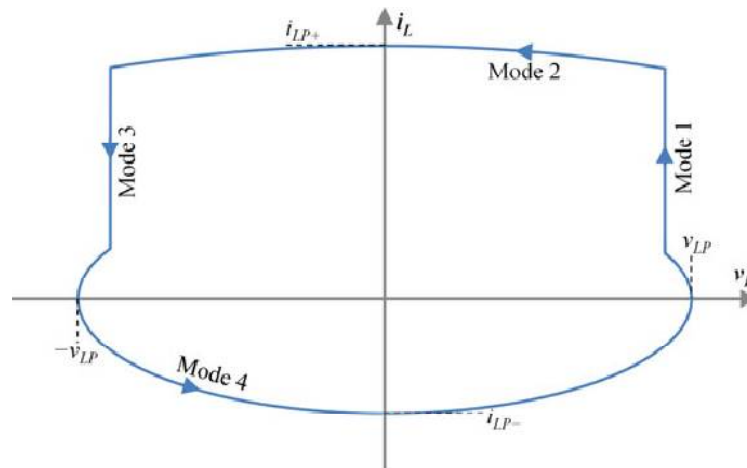


Fig. 4. State-plane diagram of the proposed converter.

The converters control scheme only requires the measurement of the main inductance voltage and current as they include the information of the input and output voltages and currents. In case of the isolated topology where the magnetizing inductance current cannot be measured directly, the transformer's primary and secondary currents should be measured and properly subtracted to reach the magnetizing inductance current. Note that by knowing the exact value of the main inductance in the isolated and nonisolated topologies, the inductance current can be easily estimated, and only the inductance voltage measurement is required. In the digital control implementation of the proposed converters, the switches may be turned ON with a delay from the exact desirable instants due to the discrete sampling. This delay may create an unwanted hard-switching operation. In order to avoid this problem, the switches can be turned ON sooner while they have negative voltages. The switches do not conduct at this time because they are RB switches and their voltages are negative. Once they become forward biased, they start conducting. By using this switching scheme, ZVS happens truly for both switches. Switch $S1$ can be turned on when $V_L(t)$ reaches its positive peak value, and switch $S2$ can be turned ON as soon as the switch $S1$ is turned OFF. As Fig. 2 shows, once $v_L(t)$ reaches its positive peak value, $i_L(t)$ passes zero in the positive direction. So, the zero crossing of $i_L(t)$ can be used as a sign to appropriately turn on switch $S1$.

In the topologies can transfer power in the reverse direction in addition to the forward direction by replacing the RB switches by bidirectional switches. The bidirectional switches can be made by using two back-to-back reverse-conducting switches in series or two RB-switches in anti-parallel. In the reverse power flow, the magnetizing inductance is charged first from the output in the negative direction. After a resonant mode, the inductance is discharged to the input by properly turning on the converter's input-side switches. Although the proposed converters are capable of bidirectional operation, more switches are required to take advantage of this feature, which partially undermines any benefit it may provide.

Fig. 5 depicts the graph of the output voltage of the proposed isolated converter versus the input reference current for the different values of the input dc voltage. According to the figure, the converter's output voltage is a function of the input reference current, and as the input reference current increases, the output dc voltage of the converter rises nonlinearly. The figure clearly illustrates that the converter works in the step-down mode of operation in the low i/p Reference current according to the desired output voltage.

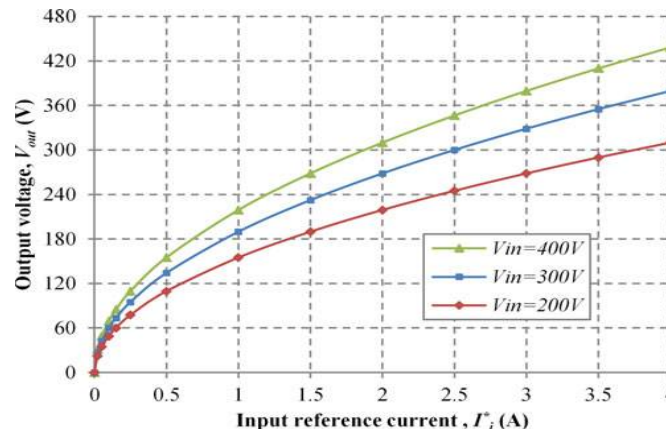


Fig. 5. Output current versus input reference current for the various values of the input voltage and $R = 120 \Omega$.

As the main inductance in the proposed topologies is rather small the dynamic response can be fast by selecting a proper bandwidth for the voltage loop.

The graph of the switching frequency, the positive peak value of the magnetizing inductance current, and the absolute value of the negative peak of the magnetizing inductance current versus L_M for the various values of C_s are shown in Fig. 6. L_M and C_s are the magnetizing inductance and total parallel capacitance seen from the secondary side of the transformer (L_M and $C_s = C_2 + C_1/n^2$). According to the figure, as the total parallel capacitance reduces, the magnitudes of the magnetizing current peak values decrease; this can be verified by considering (1) and (3). According to (10) and (11), the reduction of the total parallel capacitance also lessens the duration of the resonant modes where there is no transfer of power; consequently, i_{E1} in (1) reduces as well. It is apparent that the switching frequency increases by lessening the resonant intervals due to the reduction of the total parallel capacitance. As Fig. 6 displays, the switching frequency and the peak values of the magnetizing inductance current also depend on the magnetizing inductance value; the reduction of the magnetizing inductance increases the magnitudes of the magnetizing current peak values as well as the switching frequency. Note that the transformer's turns ratio was selected as 0.92 in this analysis, which will be discussed later.

The graph of the switching frequency and the peak values of the magnetizing inductance current versus L_M and C_s for a given operating point (see Fig. 6) can be used to design the proposed converter effectively. The magnitudes of the magnetizing current positive and negative peak values specify the conduction power loss of the switches and the transformer power loss; therefore, lowering these peak values yields smaller power losses on the switches and transformer. In addition, it is desirable to increase the switching frequency as much as possible to shrink the size of passive components. In order for the converters to run properly according to their operating principle, the main inductance voltage and current should be measured frequently in each switching cycle (at least 40–50 times). Therefore, the switching frequency should be much smaller than the sampling rate of the digital controller.

The proposed control scheme can also be implemented by using an FPGA or integrated analog design, which mainly eliminates this problem. Although the proposed partial-resonant isolated dc–dc converter can work with the transformer's turns ratio of 1 in both step-up and step-down operations, the turns ratio can be selected optimally for the optimal operation. Fig. 7 shows

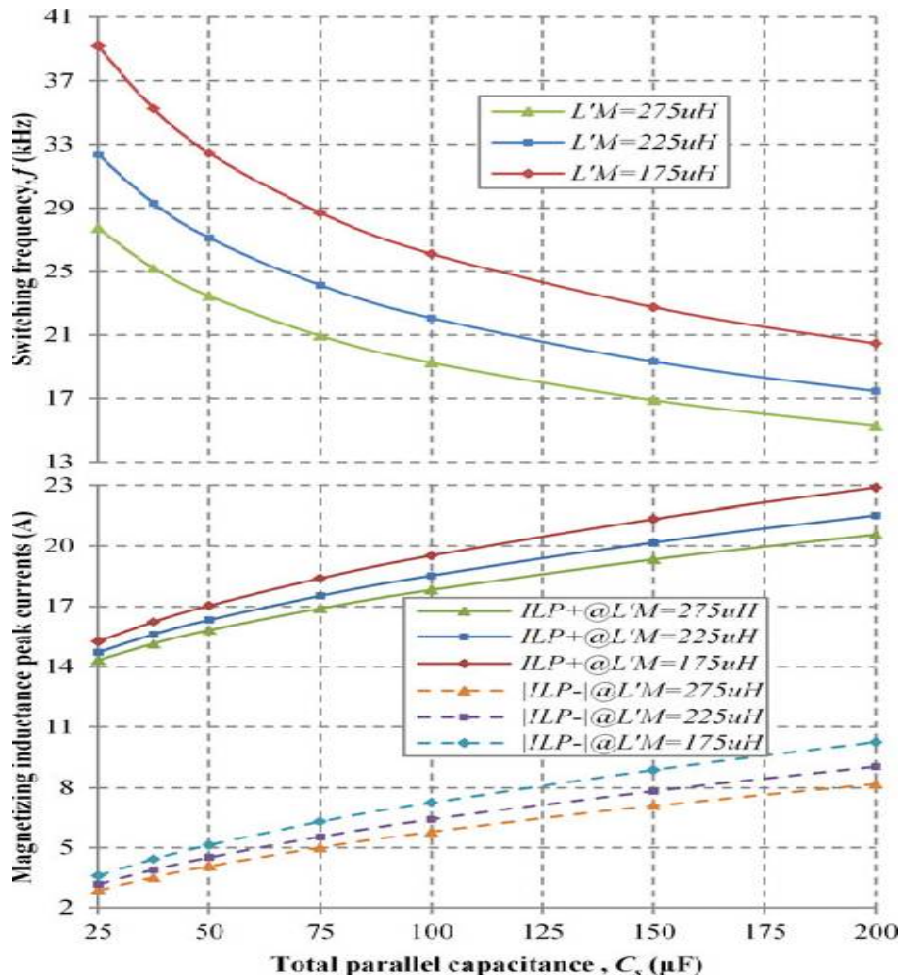


Fig. 6. Switching frequency and the magnitudes of the magnetizing current peak values versus the total parallel capacitance for various values of the magnetizing inductance, $V_{in} = 300 \text{ V}$, $R = 120 \Omega$, $n = 0.92$, and $P_{out} = 750 \text{ W}$.

The magnetizing inductance rms current, I_L , rms, versus the transformer's turns ratio for different input voltages at the given operating point. As the graph shows, the magnetizing inductance rms current reaches its lowest value when n is almost equal to 0.92 for the input voltage of 300 V (same as the output voltage). This occurs because as the turns ratio decreases from unity, the mode-3 magnetizing inductance voltage, $-V_{out}/n$, decreases. If V_{out}/n reaches the required peak value of the magnetizing inductance voltage, there is no need to leave any current in the magnetizing inductance at the end of mode 3 as stated before and $V_{LP} = V_{out}/n$. As a result, the mode-4 duration reaches its minimum value [note the second term in (11)], and the converter operates more efficiently. Decreasing n lower than the optimized value will cause an increase in V_{LP} , which lengthens the mode-4 duration. As Fig. 7 reveals, the optimum turns ratio depends on the input voltage; in the case of a different input voltage, the optimum turns ratio can be found by multiplying 0.92 by the output-input voltage ratio.

International Journal of Advanced Research in Electrical, Electronics and Instrumentation Engineering

(An ISO 3297: 2007 Certified Organization)

Vol. 5, Issue 7, July 2016

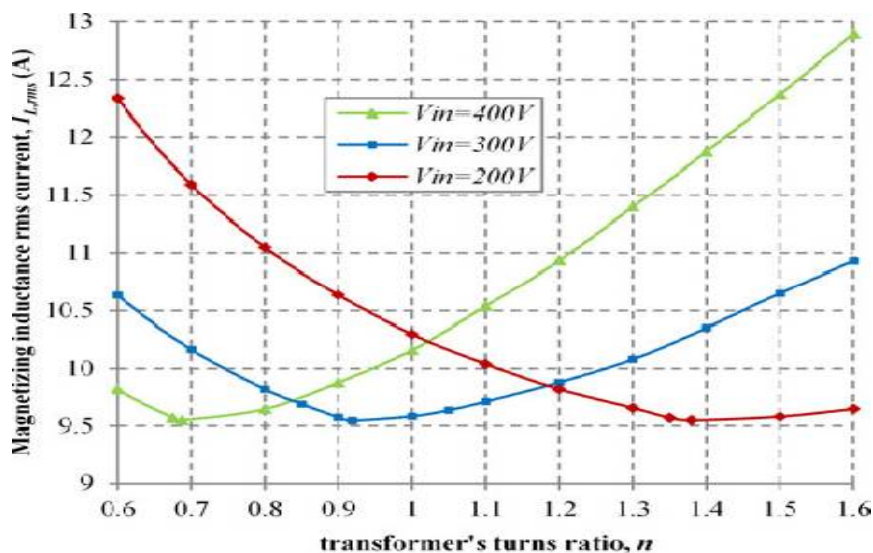
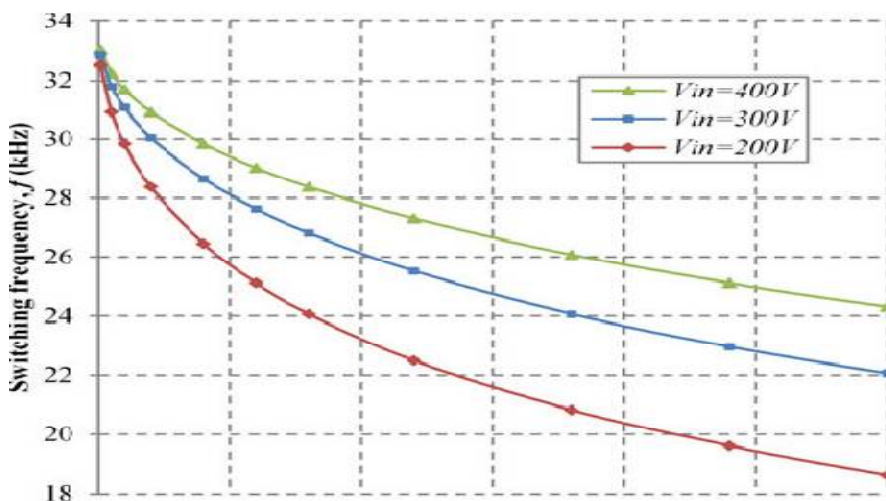


Fig. 7. Magnetizing inductance rms current versus the transformer's turns ratio for various input voltage values, $R = 120 \Omega$, $L_M = 225 \mu H$, $C_S = 100 \text{ nF}$, $V_{LP} = 1.1 V_{in}$, and $P_{out} = 750 \text{ W}$.

In Fig. 8 shows the switching frequency and the magnitudes of the magnetizing current peak values versus the output power for different values of the input voltage. According to the figure, the positive peak value of the magnetizing inductance current is completely dependent on the output power, and as the output power reduces, I_{LP+} decreases almost linearly. This occurs because as the output power drops, the input reference current should decrease accordingly.



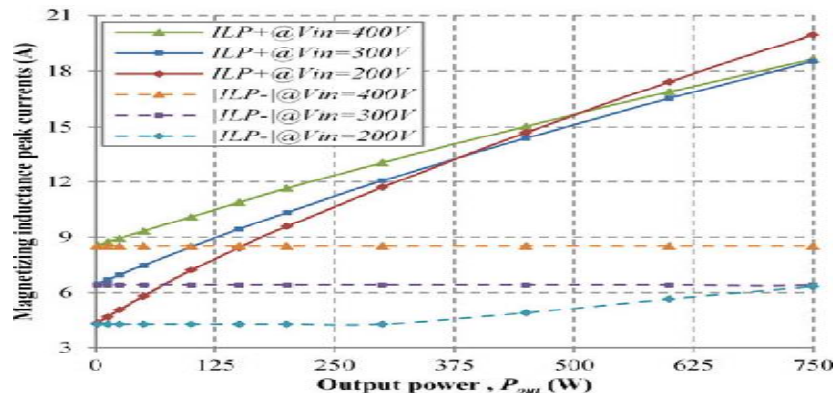


Fig. 8. Switching frequency and the magnitudes of the magnetizing current peak values versus the output power for various input voltage values, $R = 120 \Omega$, $L_M = 225 \mu\text{H}$, $C_s = 100 \text{ nF}$, and $n = 0.92$.

Therefore, the time lengths of modes 1 and 3 decrease, which results in the reduction of I_{E1} in (1) and consequently I_{LP+} . In addition, the reduction in duration of the odd-numbered modes results in the increase of the switching frequency. Note that according to (3), I_{LP+} does not depend on the output power, but it may depend on the input voltage (V_{LP} should be higher than the input voltage). The switching frequency and the magnitudes of the magnetizing current peak values at a very small amount of the output power.

According to Fig. 8, the change of the input dc voltage at a given output power affects the operating parameters of the proposed converter moderately. Although the increment of the input voltage at any given power increases the switching frequency, the change of the peak values of the magnetizing inductance current depends on the output power and input voltage values at the operating point of the converter.

IV. SIMULATION RESULTS

Here the performance of the isolated partial-resonant converter DC-DC buck-boost and flyback converter will be evaluated during simulations. These results will be compared with the experimental results of the original configuration.

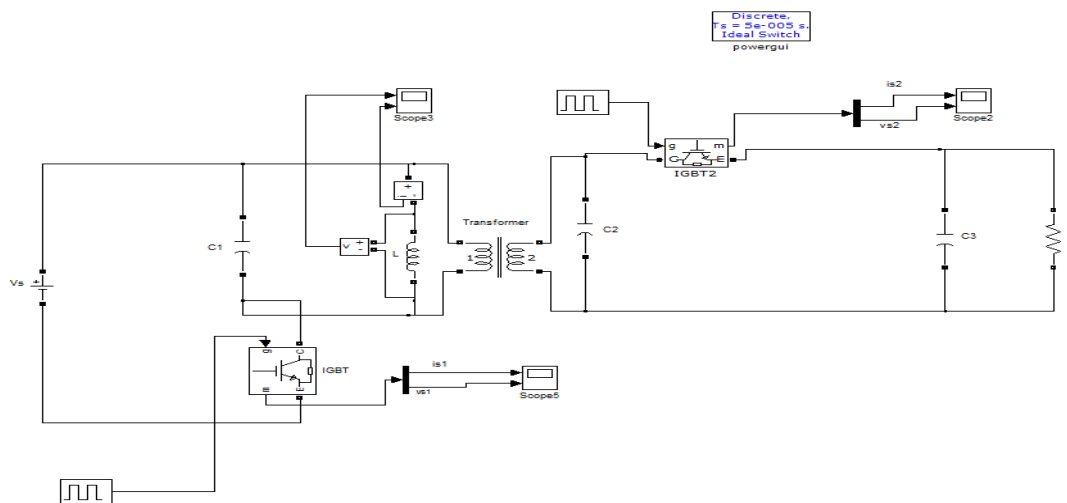


Fig. 9(a) Simulink Model of New generation buck-boost and flyback dc-dc converter.

International Journal of Advanced Research in Electrical, Electronics and Instrumentation Engineering

(An ISO 3297: 2007 Certified Organization)

Vol. 5, Issue 7, July 2016

The simulink model for a new generation of buck-boost and flyback dc-dc converter power flow is shown in Fig. 9(a)

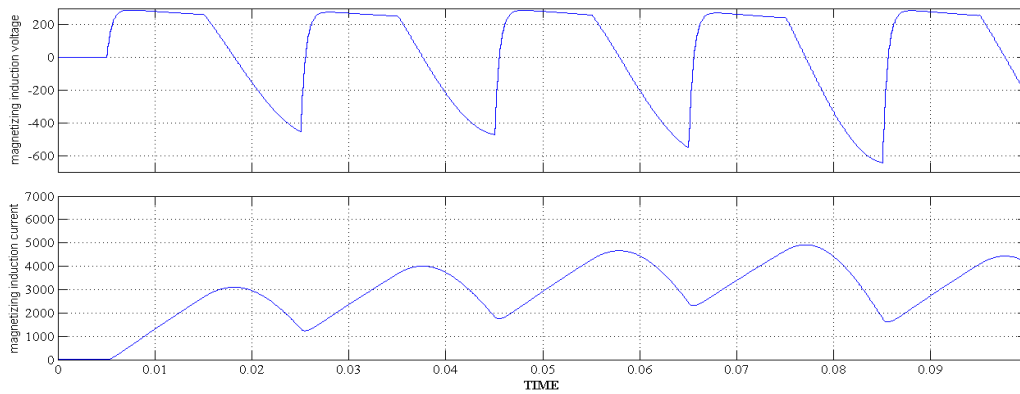


Fig. 10. Results with 300 V input at 750 W. Top: magnetizing inductance voltage (300 V/div), and bottom: magnetizing inductance current (20 A/div) versus time (12 μ S/div).

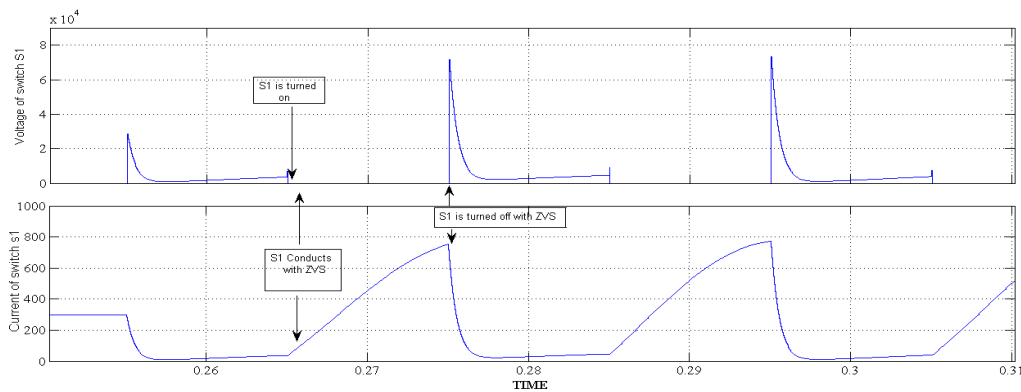


Fig. 11. The results with 300 V input at 750 W. Top: voltage of switch S1 (400 V/div), and bottom: current of switch S1 (20 A/div) versus time(5 μ S/div).

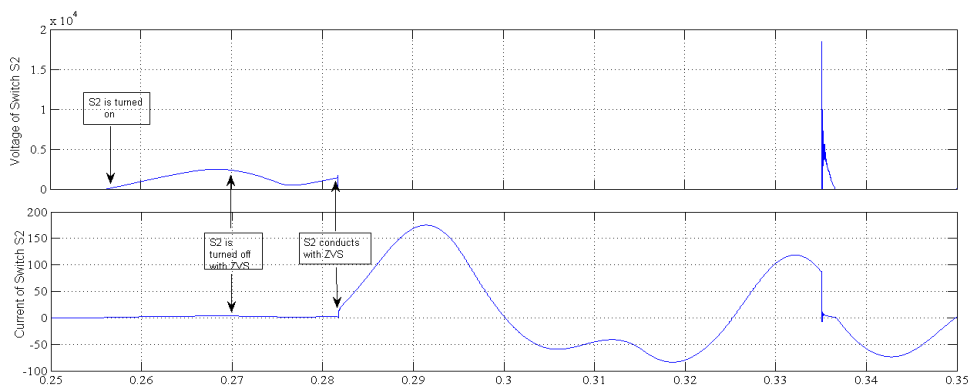


Fig. 12. The results with 300 V input at 750 W. Top: voltage of switch S2 (400 V/div), and bottom: current of switch S2 (20 A/div) versus time(5 μ S/div).

International Journal of Advanced Research in Electrical, Electronics and Instrumentation Engineering

(An ISO 3297: 2007 Certified Organization)

Vol. 5, Issue 7, July 2016

The simulink model for a new generation of buck-boost and flyback dc-dc converter power flow is shown in fig. 9(b)

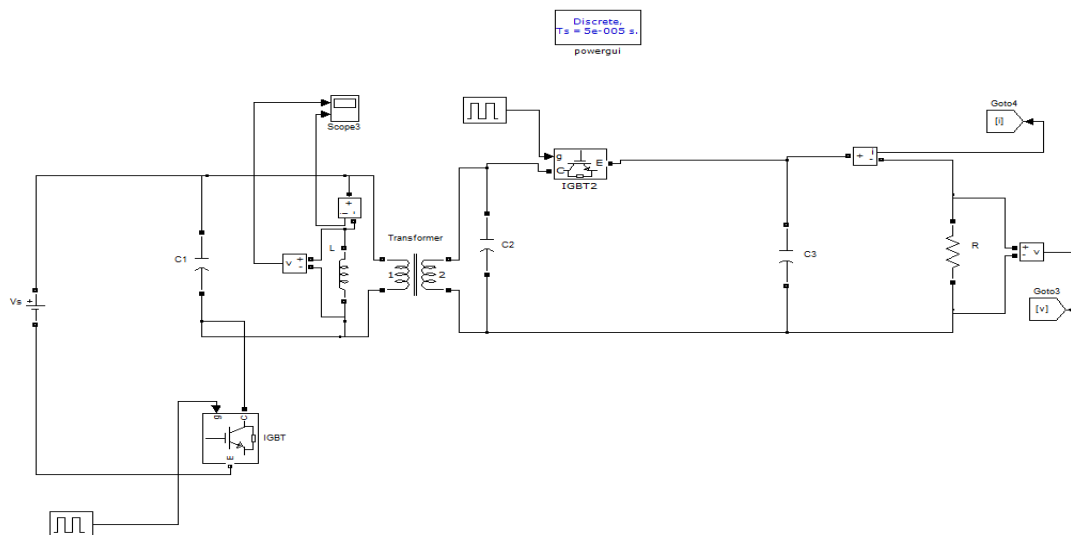


Fig. 9(b) Simulink Model New generation buck-boost and flyback dc-dc converter.

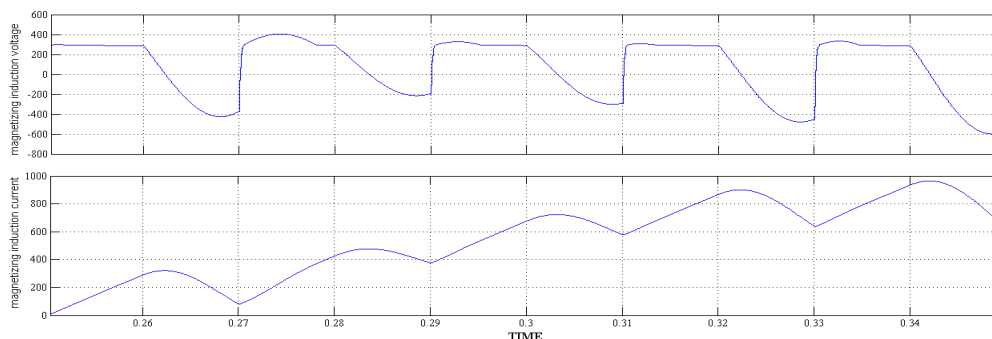


Fig. 13. The results with 300 V input at 375 W. Top: magnetizing inductance voltage (300 V/div), and bottom: magnetizing inductance current (20 A/div) versus time (12 μ S/div).

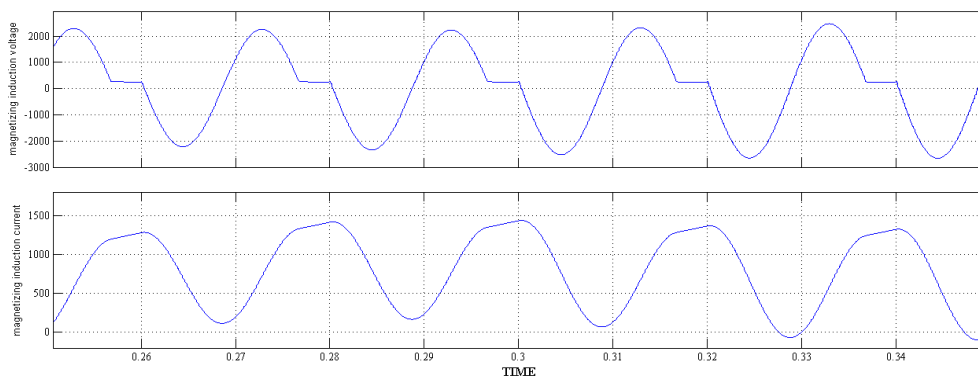


Fig. 14. The results with 300 V input at 75 W. Top: magnetizing inductance voltage (300 V/div), and bottom: magnetizing inductance current (20 A/div) versus time (12 μ S/div).

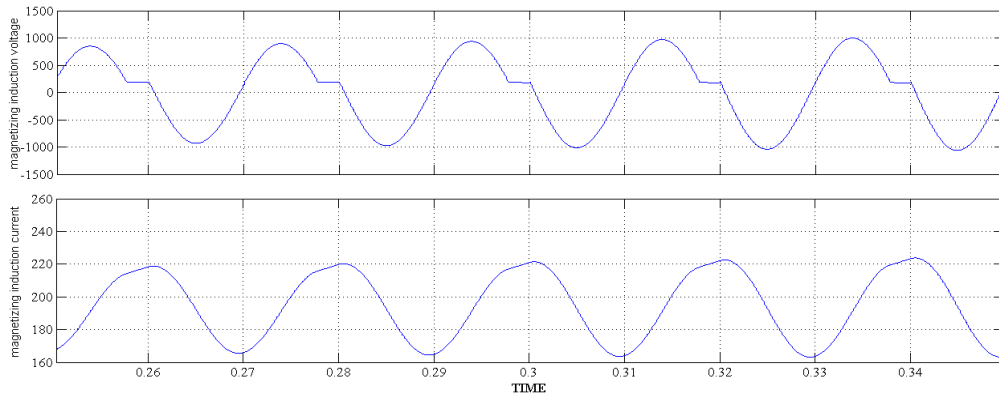


Fig.15. The results with 200 V input at 750 W. Top: magnetizing inductance voltage (300 V/div), and bottom: magnetizing inductance current (20 A/div) versus time (12 μ S/div).

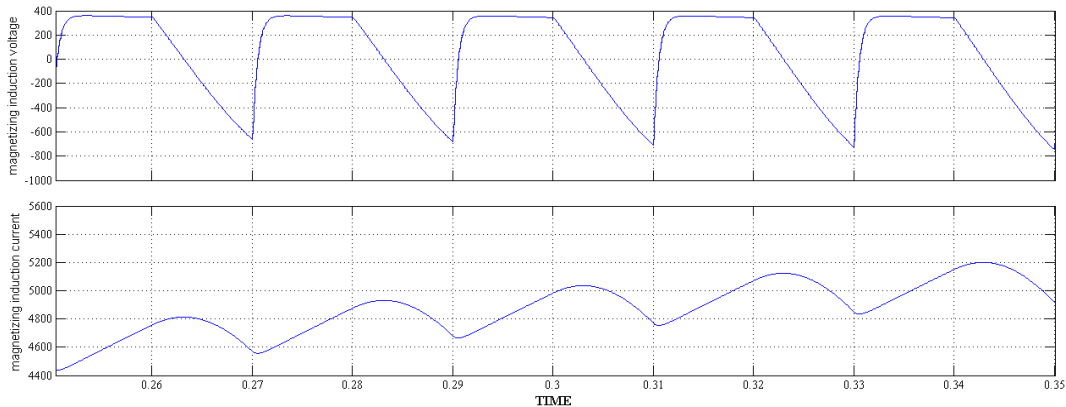


Fig.16. The results with 400 V input at 750 W. Top: magnetizing inductance voltage (300 V/div), and bottom: magnetizing inductance current (20 A/div) versus time (12 μ S/div).

V. CONCLUSION

A new generation of soft- switched buck-boost dc-dc converter was introduced in this project. The partial-resonant network is composed of a small inductor in parallel with a small ac capacitor. The main role of the inductor is to transfer power by charging from the input and discharging to the output or vice versa. The parallel capacitor creates partial Resonances to realize zero-voltage turn-on and turn-off for the converter's switches. The inductor can be simply replaced by an air-gapped high-frequency transformer to achieve galvanic isolation. Multiple results were presented to demonstrate the effective performance of the proposed topology in different operating conditions This project has been developed by using Matlab/Simulink software and studied the results.

REFERENCES

- [1] R. Erickson and D. Maksimovic, *Fundamentals of Power Electronics*, 2nd ed. New York, NY, USA: Kluwer, 2004.
- [2] I. Aksoy, H. Bodur, and A. F. Bakan, "A new ZVT-ZCT-PWM DC-DC converter," *IEEE Trans. Power Electron.*, vol. 25, no. 8, pp. 2093–2105, Aug. 2010.
- [3] K. H. Liu and F. C. Lee, "Zero-voltage switching technique in DC/DC converters," *IEEE Trans. Power Electron.*, vol. 5, no. 3, pp. 293–304, Jul. 1990.



International Journal of Advanced Research in Electrical, Electronics and Instrumentation Engineering

(An ISO 3297: 2007 Certified Organization)

Vol. 5, Issue 7, July 2016

- [4] J. Dudrik and N. D. Trip, "Soft-switching PS-PWM DC-DC converter for full-load range applications," *IEEE Trans. Ind. Electron.*, vol. 57, no. 8, pp.2807–2814, Aug. 2010.
- [5] H. Rongjun and S. K. Mazumder, "A soft-switching scheme for an iso-lated DC/DC converter with pulsating DC output for a three-phase high-frequency-link PWM converter," *IEEE Trans. Power Electron.*, vol. 24, no. 10, pp. 2276–2288, Oct. 2009.
- [6] F. C. Lee, "High-Frequency quasi-resonant and multi-resonant converter technologies," in *Proc. 14th Annu. Conf. Ind. Electron. Soc.*, Oct. 1988, vol. 3, pp. 509–521.
- [7] G. Hua, C. S. Leu, and F. C. Lee, "Novel zero-voltage-transition PWM converters," in *Proc. IEEE Power Electron. Spec. Conf.*, 1992, pp. 55–61.
- [8] W. J. Gu and K. Harada, "A novel self-excited forward DC-DC converter with zero-voltage-switched resonant transitions using a saturable core," *IEEE Trans. Power Electron.*, vol. 10, no. 2, pp. 131–141, Mar. 1995.
- [9] R. Watson, F. C. Lee, and G. Hua, "Utilization of an active-clamp cir-cuit to achieve soft switching in flyback converters," *IEEE Trans. Power Electron.*, vol. 11, no. 1, pp. 162–169, Jan. 1996.
- [10] L. Jong-Jae, J. Kwon, K. Eung-Ho, and B. Kwon, "Dual series-resonant active-clamp converter," *IEEE Trans. Ind. Electron.*, vol. 55, no. 2, pp. 699–710, Feb. 2008.
- [11] J. A. Sabate, V. Vlatkovic, R. B. Ridley, and F. C. Lee, "High-voltage, high-power, ZVS, full-bridge PWM c onverter employing an active snub-ber," in *Proc. Appl. Power Electron. Conf. Expo.*, Mar. 1991, pp. 158–163.
- [12] M. K. Kazimierczuk, N. Thirunarayan, and S. Wang, "Analysis of series-parallel resonant converter," *IEEE Trans. Aerosp. Electron. Syst.*, vol. 29, no. 1, pp. 88–98, Jan. 1993.
- [13] D. Fu, F. C. Lee, Y. Qiu, and F. Wang, "A novel high-power-density three-level LCC resonant converter with constant-power-factor-control for charging applications," *IEEE Trans. Power Electron.*, vol. 23, no. 5, pp.2411–2420, Sep. 2008.
- [14] Y. Gu, Z. Lu, L. Hang, Z. Qian, and G. Huang, "Three-level LLC series resonant dc/dc converter," *IEEE Trans. Power Electron.*, vol. 20, no. 4, pp.781–789, Jul. 2005.
- [15] X. Fang, H. Hu, F. Chen, U. Somani, E. Auadisian, J. Shen, and I. Batarseh, "Efficiency-oriented optimal design of the LLC resonant converter based on peak gain placement," *IEEE Trans. Power Electron.*, vol. 28, no. 5, pp. 2285–2296, May 2013.
- [16] H. Keyhani, H. A. Toliyat, M. Todorovic, R. Lai, and R. Datta, "An iso-lated resonant AC-Link Three-Phase AC-AC converter using a single HF transformer," *IEEE Trans. Ind. Electron.*, 2014.
- [17] W. A. Roshen, "Fringing field formulas and winding loss due to an air gap," *IEEE Trans. Magn.*, vol. 43, no. 8, pp. 3387–3394, Aug. 2007.
- [18] M. Chen and J. Sun, "Reduced-order averaged modeling of active-clamp converters," *IEEE Trans. Power Electron.*, vol. 21, no. 2, pp. 487–494, Mar. 2006.

BIOGRAPY



Ch. Kranthi Kumar received B.Tech degree in Electrical and Electronics Engineering under Jawaharlal Nehru Technological University, Anantapuram, India in 2013. Currently he is pursuing M.Tech in Power Electronics in, Narayana Engineering College, Gudur, A.P, India. His research areas of interests are development in Power Electronics for low power applications & Implementation of fuzzy systems in low power drives.



Dr. G. JAYA KRISHNA received B.Tech, M.Tech and Ph.D degrees in Electrical Engineering from Jawaharlal Nehru Technological University, Anantapuram, India in 1993, 2004 and 2013 respectively. Currently he is working as Professor & Head of Department of Electrical and Electronics Engineering, Narayana Engineering College, Gudur, A.P, India. His research interests include Power Quality, Electrical drives and Power Systems. He is life member of ISTE.